P4.21

MULTISCALE ANALYSES OF MOISTURE TRANSPORT BY THE CENTRAL PLAINS LOW-LEVEL JET DURING IHOP

Edward I. Tollerud[1], Brian D. Jamison[1,2], Fernando Caracena[1], Steven E. Koch[1], Diana L. Bartels[1], R. Michael Hardesty[3], Brandi J. McCarty[3], Christoph Kiemle[4], and Gerhard Ehret[4]

[1]NOAA Research-Forecast Systems Laboratory, Boulder, CO
[2]Cooperative Institute for Research in the Atmosphere, Fort Collins, CO
[3]NOAA Research-Environmental Technology Laboratory, Boulder, CO
[4]German Aerospace Center (DLR), Germany

1. INTRODUCTION

During the International H_2O Project (IHOP) in the Southern U.S. Central Plains (Weckwerth *et al.* 2004) in May and June 2002, aircraft missions on June 3 and June 9 2002 made detailed lidar and dropsonde observations of intense phases of the low-level jet (LLJ) . Combined with standard and enhanced operational observations (primarily radiosondes and profilers) and other ground-based research observations, data from these missions represent an unprecedented opportunity to describe moisture transport in the LLJ at scales ranging from the synoptic scales resolved by the radiosonde network to sub-mesoscale features in the moisture and wind fields observed by airborne lidar instruments.

Two questions immediately present themselves: (1) Do focused observations at exceptionally high resolution provide details critical to our physical understanding of the LLJ; and (2) would inclusion of these details in model initialization fields significantly alter model-generated forecasts of LLJ evolution, transport, and subsequent precipitation generation? A practical way of stating (1) is: do small-scale correlations between moisture and wind fluctuations within the LLJ significantly alter larger-scale estimates of LLJ moisture transport? To illustrate this possibility, we present vertical sections across the LLJ of wind, moisture, and resulting moisture transport from multiple observation sets including radiosonde only, dropsondes, and simultaneous lidar measurements of moisture and wind. Cumulative transport through the sections will also be presented to estimate possible scale effects. In future work, we will directly address (2) by comparing analyses and numerical predictions from a control run of the Weather Research and Forecasting Model (WRF) made with operational datasets with an otherwise parallel analysis and forecast that have the advantage of input from research dropsonde observations and other research data.

Corresponding author address: Edward Tollerud, NOAA/FSL/FS1, 325 Broadway, Boulder, CO 80305-3328. E-mail: edward.tollerud@noaa.gov. Tel: 303-497-6127.

2. SCIENTIFIC OBJECTIVES

The focus of IHOP was on the characterization of the water vapor field. However, improved characterization of the transport of moisture may also provide important improvements in QPF skill. For example, Guo *et al.* (2000) found that assimilation of wind data from the NOAA Profiler Network produced a greater positive impact on the vertical profile of water vapor than assimilation of either the surface dew point or the GPS vertically integrated water vapor measurements. The southerly low-level jet (LLJ) is the most effective mechanism for advecting low-level moisture into the central United States, and is thereby responsible for increasing the potential for deep moist convection and heavy precipitation. Supply of moisture from the Gulf of Mexico by the LLJ to the location of an existing low-level boundary such as a warm front results in lifting of moist air and often the development of mesoscale convective systems (MCSs). Augustine and Caracena (1994) found that one of the precursors foreshadowing the occurrence of MCSs over the central United States was an LLJ transporting moisture toward the warm side of a frontogenetic boundary at 850 hPa in an area where the troposphere is being destabilized by the approach of a short wave trough. Higgins *et al.* (1997) estimate that the contribution of the LLJ to low-level moisture transport is almost 50% above average non-LLJ values. The depth, width, and magnitude of moist inflow, and the moisture convergence profile, are all functions both of the water vapor and the wind fields. The extent to which such factors determine if an MCS will form on a given day, as well as their influence on the MCS intensity, longevity, and rainfall production after it forms, need to be understood.

Because MCSs produce a substantial fraction of rainfall in regions where they are frequent (Fritsch *et al.* 1986), better understanding and observation of the detailed structure of the water vapor field within the LLJ could potentially lead to improvement in warm season QPF over much of the central U.S. Demonstration of this improvement would be, at least in part, a result of better resolution of the structure of the LLJ by assimilating the special IHOP observations in high-resolution models. Current operational models rely primarily on coarsely-spaced rawinsonde observations supplemented by wind profiler and ACARS winds to identify the LLJ, which is apparently sufficient to predict the large-scale structure and dynamics of the LLJ fairly well. However, smaller-scale LLJs (or "jetlets") may help to spawn and nurture MCSs attended by catastrophic flash floods and/or severe weather (Koch *et al.* 1998). Some hint of this variability is contained in the early observations of Hoecker (1963), which indicated large changes in the vertical structure of the LLJ on an hourly time scale. Spatially, however, those measurements were fairly coarse, with an average spacing of ~70 km along a single east-west cross section. Studies in the United Kingdom have also confirmed the existence of jetlets ahead of strong cold fronts (Browning and Pardoe 1973). Model studies during the last 30 years that have investigated the development and dynamics of the LLJ and its connection to severe weather have suggested a dynamical linkage between the upper-level jet and the LLJ (Brill *et al.* 1985; Uccellini *et al.* 1987), as well as the idea that low-level jetlets might be generated as the result of a geostrophic adjustment process ensuing from latent heating in organized deep convection (Koch *et al.* 1998). Because the observations are spatially coarse, they are deficient in providing a detailed description of the structure or behavior of the LLJ; thus, it can be difficult to verify these simulated structures. It is not surprising, therefore, that numerical models do not provide a complete description of the LLJ (Anderson and Arrit 2001).

3. DATA AND EXPERIMENTAL DESIGN

One key objective of the two morning LLJ flights (June 3 and 9) during IHOP was to examine how the LLJ evolves as the boundary layer develops in the morning hours before deep convection forms. For example, the LLJ might suddenly weaken and/or reform at a higher altitude as the stable nocturnal boundary layer disappears. Jetlets or other small scale features may develop in response to horizontal inhomogeneities in surface sensible heating arising from heterogeneous fields of soil moisture or other surface attributes. These and other intriguing possibilities need to be investigated and well understood before they can be predicted reliably and realistically. An important aspect of these investigations is a determination of the role that motions of various scales play in the transport of moisture by the LLJ.

To gather the necessary observations for these investigations, the following observational strategies were employed. Two dropsonde aircraft (the DLR Falcon and a Learjet) flew box patterns chosen to bracket the predicted location of the LLJ on a morning when a strong LLJ is predicted. An example is the box pattern flown on 9 June (Fig. 1).

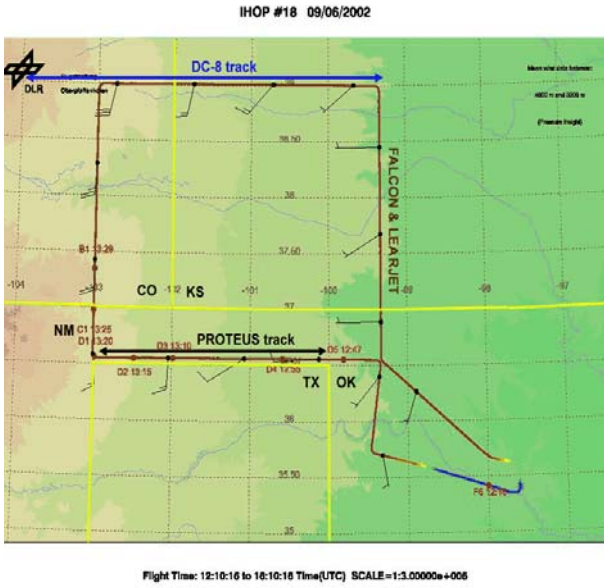

Fig. 1. Flight pattern for the 9 June LLJ flights of the DLR Falcon and Learjet (brown lines) over western Kansas and adjoining states. LASE measurements were made along the blue DC-8 track, and NAST measurements were made by the PROTEUS along the double-ended black arrow.

The box size, location, and orientation were also chosen with regard to possibilities for computing full-domain moisture budget terms (see Conclusions below). Mission days were selected during clear-to-partly cloudy conditions since lidar systems were flown. The NCAR GPS dropwindsonde flown on these aircraft provide wind accuracies of 0.5 - 2.0 m s-1 with an impressive vertical resolution of ~5 m and detailed humidity measurements with accuracy of at least 2% all the way down to the surface

(Hock and Franklin 1999). The aircraft thus provided full wind and moisture profiles below flight altitude at approximately 55-km intervals along the periphery of the flight box. It was the original intent to have each aircraft complete the full rectangular circuit, refuel, and then repeat the circuit a second time. However, as described below, experimental difficulties forced changes in this strategy.

A smaller-scale description of moisture and airflow around the rectangular domain were provided by the DLR Falcon aircraft lidar measurements of winds (from High-Resolution Doppler Lidar, HRDL) and specific humidity (from the downward-pointing Differential Absorption Lidar, DIAL). Only winds transverse to the aircraft flight path were measured by the HRDL. Additional moisture observations were available along part of the flight patterns from the Lidar Atmospheric Sensing Experiment (LASE) on the NASA DC-8 and the NPOESS Airborne Sounder Testbed (NAST) on the NASA Proteus research aircraft. The major strength of lidars is their ability to provide very detailed vertical profiles unrestricted by ground clutter, but they are restricted in their utility to the absence of clouds and precipitation, and have limited range due to attenuation effects. With these measurements, water vapor variability within the domain in the middle to lower troposphere can be calculated at small (lidar-measured) scales in the optically clear air to complement the larger effective scale of the dropsondes available in all weather conditions. The combined use of the DIAL, LASE, NAST, and HRDL allows us to address the question of the scale-dependence of the moisture transport in the presence of a low-level jet.

To provide the large-scale setting to the LLJ, the operational datastream of radiosonde, profiler, and surface observations were analysed. For the two MLLJ cases during IHOP, 3-hourly special radiosonde launches were also available at conventional NWS sites.

4. RESULTS FROM THE 9 JUNE LLJ CASE

4.1 Flight Plan and Observations

The flight plan for this case is shown on Fig. 1. Its location and orientation was designed to capture the predominantly N-S LLJ centered on the Oklahoma panhandle through central Kansas on this morning. Flights started shortly after 1200 UTC, with the Learjet beginning drops at the Northwest corner, and the Falcon beginning its flight at the Southeast corner. Although two full aircraft circuits were intended, the Falcon developed tire problems and could only fly one circuit, which was complelted by about 1450 UTC. The second Learjet flight was from 1650-1850 UTC. Most of the dropsonde releases during these circuits were successful. Some loss of DIAL data on the Falcon occurred near the northeast corner; attempts to retrieve that data are ongoing.

In addition, LASE data from the DC-8 were obtained from about 1415 to 1715 UTC over the northern leg (see Fig. 1). The DC-8 and Falcon were flying the same path at the time but in opposite directions, making their most closely matched observations around 1415 UTC. The southern leg of the flight pattern was also traversed by the PROTEUS aircraft collecting NAST data from 1248 to 1600 UTC. The southern flight leg passed over other special ground based IHOP instruments operating at the time, such as the S-POL radar, at about its mid-point.

4.2 Multiscale Transport Estimates

Moisture transport orthogonal to the rectangular flight box ($\mathbf{v}_n$ x q) by different scales of motion is shown here as sections along the northern and southern legs of the flight pattern of Fig. 1. Although the LLJ was intersected along both legs, a more complete set of aircraft observations were obtained along the northern leg.

Large-scale estimates (otherwise interpretable as the picture presented by operational data platforms) of moisture transport by the v wind component (used here because it is transverse to the the east-west-oriented northern and southern flight legs) are shown in Fig. 2. Compared to the sections of dropsonde-observed transports along this same leg (Fig. 3), the large scale transports at the jet core are slightly larger (350 vs. 250) but not as focused. However, comparison of the two sections of transport estimates are complicated by the difference in observation periods (nominally 1200 UTC for the radiosondes, and between 1350 and 1430 UTC for the dropsondes). Future analysis of the Learjet dropsonde observations (which were made along the northern track closer in time to 1200 UTC) will offer a better comparison. However,these latter observations are without supporting airborne lidar measurements, limiting their usefulness for other purposes.

Figures 4 and 5 show, respectively, vertically-integrated and mass-weighted moisture transports between the surface and flight level along the northern and southern legs computed from dropsonde

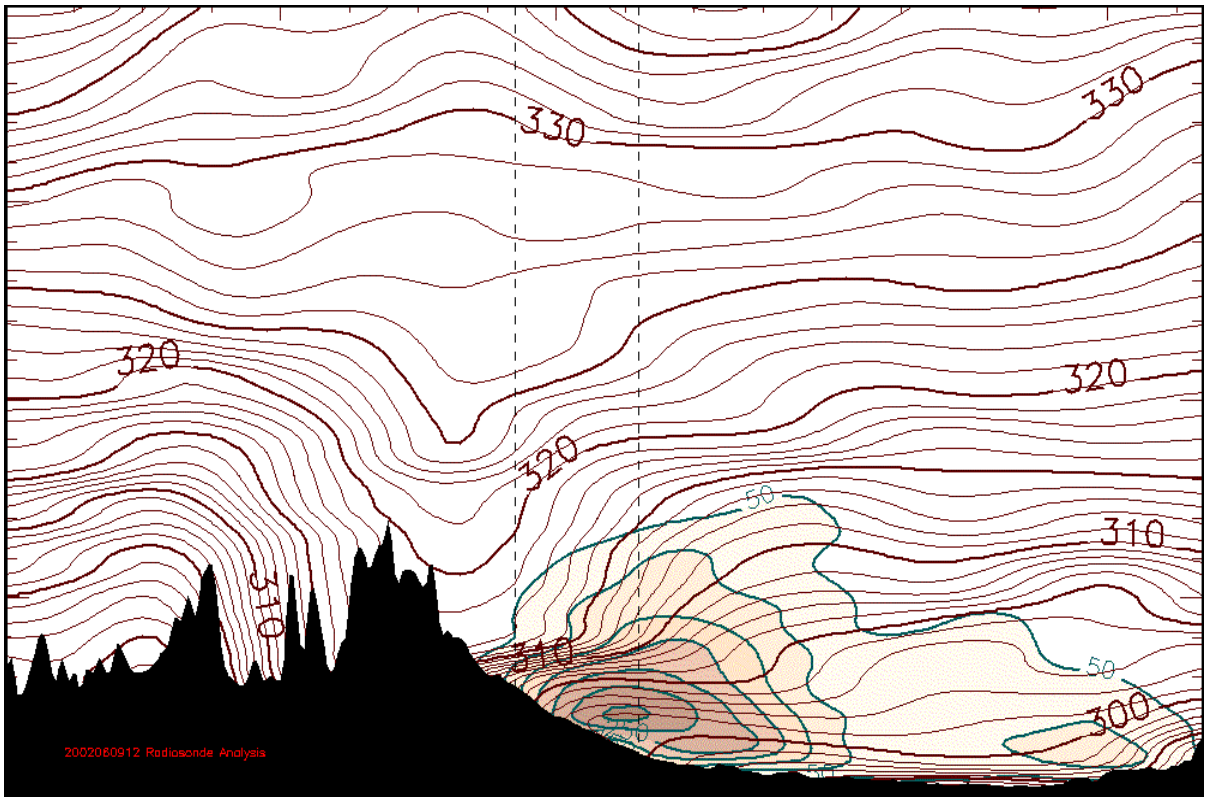

Fig. 2. Moisture transport (v x q) (shaded, with contour interval of 50 $gkg^{-1}ms^{-1}$) transverse to the northern leg of the 9 June flight box. Estimates are based on analysis of radiosonde observations at 1200 UTC. Vertical dashed lines denote west and east ends of the northern leg. Potential Temperature contours also shown (contour interval of 1°K).

observations, and a vector representation of this transport along all legs of the mission. Vertically-integrated lidar measurements are not yet available. It is apparent that transport into the measurement domain through the southern section is roughly matched by transport out of the domain through the northern section. The increase in transport along the northern leg from west to east is an effect of increasing moisture and windspeed (the core of the jet is markedly stronger near the northeast corner of the flight box). Along the southern leg, where there is less change in wind magnitude, the increase in transport is largely due to longitudinal variation in moisture.

The profiles of moisture transport within a column in Fig. 6 provide more detail and also allow comparison with parallel measurements made by the combination of lidar instruments (the HRDL and DIAL) on the DLR Falcon. To synchronize the time of measurement of the various observations as much as possible, this comparison is made for a point along the southern leg sampled by the Falcon just after 1250 UTC. There is surprising agreement between the platforms, both in vertical distribution and magnitude. Since lidar values along this southern leg were attenuated before they reached the ground, it is possible that measurements at the height of maximum jet velocity and below, when (and if) they can be retrieved, will show flux values larger than the other two platforms.

The curve of along-track moisture transport (in this case, transport by the u-component of the wind) as specified by dropsondes is included to help assess the impact of having just one component of lidar-observed winds. At lower levels, the winds are very nearly meridional, so that along-track transports are small. However, as the wind turns with height, the other component of transport approaches the transverse component in magnitude. We thus conclude that estimates based solely on lidar winds and moisture measurements will significantly underestimate the total transports at some loca-

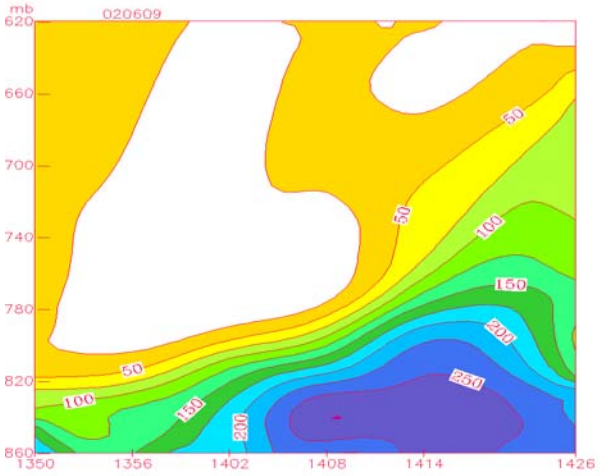

Fig 3. Dropsonde-observed moisture transport (v x q) normal to the northern leg of the 9 June flight box. Units are as in Fig. 2, but with contour intervals of 25. Times along x-axis denote dropsonde release times (UTC); distances between releases is about 55 km.

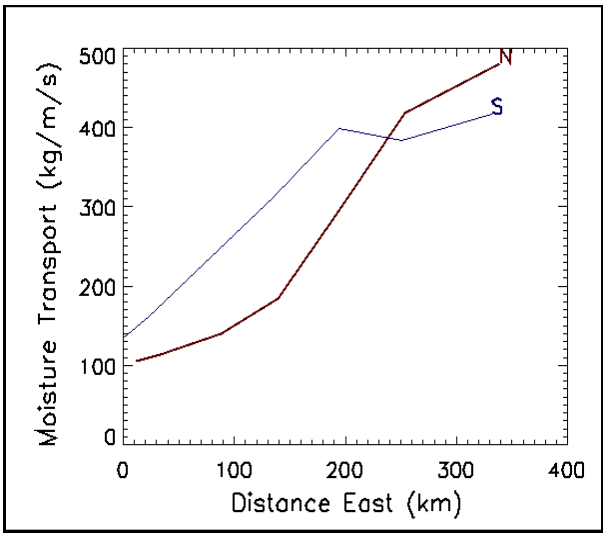

Fig. 4. Vertically-integrated density-weighted moisture transport normal to the flight track between the surface and aircraft flight level computed from dropsondes along the south (blue) and north (red) legs of the 9 June DLR Falcon flight path.

tions and heights along the legs of the aircraft flight tracks.

Further examination of measurements of dropsonde launches (especially those made by the Learjet) along all legs of both cases should help to answer the questions raised by these preliminary comparisons.

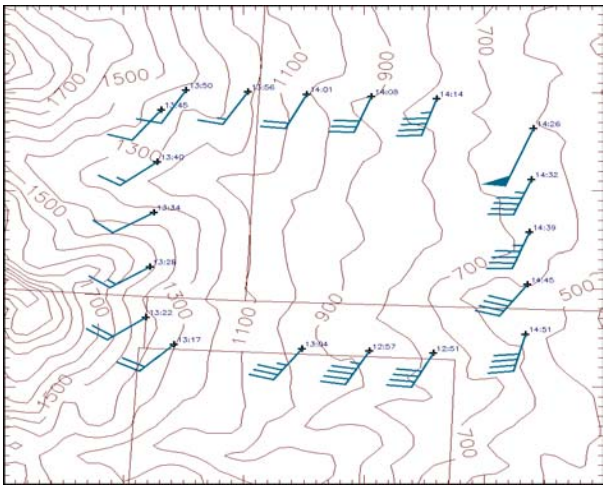

Fig. 5. Vertically-integrated density-weighted moisture transport along the perimeter of the 9 June mission flight path computed from DLR Falcon dropsondes. Multiply vector units by ten to get transport in kg/m/s. Terrain values are displayed in meters, with a contour interval of 100 m.

5. CONCLUSIONS AND NEXT STEPS

The geometry and other flight characteristics of the LLJ missions suggest the applicability of a moisture budget analysis. Indeed, as indicated previously, the mission flight patterns were partly chosen to make this a possibility. Thus, future efforts to analyze data from these missions will include computations of moisture budget terms. A methodology for the computation of the horizontal transport terms of this budget, for example, is readily apparent in Fig.5; the integrated normal component vectors along the perimeter of the box will give the net gain/loss of moisture within the box. Previous moisture budget studies over the central U. S. have been aimed at large scales that can be adequately resolved with the existing radiosonde network (Roads *et al.* 1994). Imbalances in these budgets have been attributed to observational limitations, especially to inadequate time resolution of the twice-per-day radiosonde releases. For a phenomenon like the LLJ with strong diurnal variation, this difficulty is particularly troublesome. Kuo and Anthes (1984) simulated the moisture budget for the central U.S. during Project SESAME and found that average values for moisture budget terms corresponded well to observations. IHOP offers some real advantages but suffers some disadvantages as well. On the positive side, the very detailed moisture flux measurements and surface observations will provide

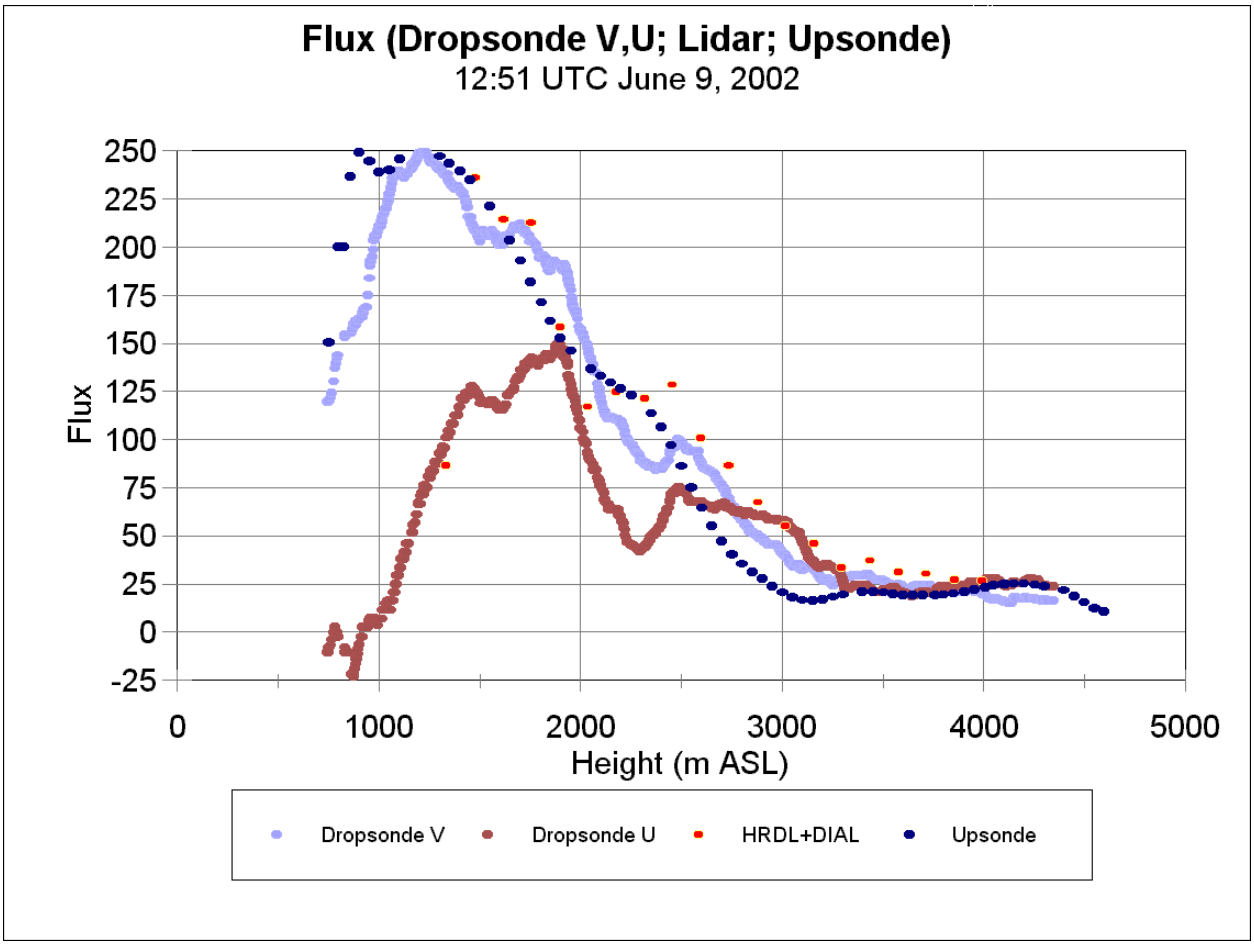

Fig. 6. Comparison of cross-track transports (v x q; units as in Fig. 2) observed at 1251 UTC near the eastern end of the southern leg of the flight box on 9 June . Brown curve describes along-track transports (u x q) observed by dropsondes but unmeasurable by the DLR Falcon HRDL system.

estimates of atmospheric transports and surface moisture fluxes needed to correct the broad-brush large-scale estimates. Nevertheless, the mix of observation types over a rather limited domain presents a challenging problem for assimilation and analysis of data into a form suitable for budget calculations.

With these assets and liabilities in mind, we intend to pursue a limited budget study that is specifically focused on the LLJ. Three natural scales emerge from the array of IHOP observations. Synoptic scale circulations can be diagnosed by the expanded radiosonde and conventional observations of the operational array. Moving down in scale, the dropsonde observations and profiler sites describe scales close to the size of the IHOP domain and the width of the LLJ, but are not suited for fine-scale flux measurements. This third scale can be described, however, by the lidar and other specialized observing systems over smaller regions within the IHOP domain. Our budget computations will concentrate on the middle of these scales, with input from smaller scales to estimate the magnitude of subscale covariances to the budget. We believe that dropsonde observations will provide accurate estimates of cross-boundary moisture fluxes at time and space scales relevant to the LLJ. On the other hand, difficulties with closure of this moisture budget are obvious. For instance, direct observations of cloud water (if any) moving out of the dropsonde array will not be available, nor will direct observations of the vertical transport of moisture. However, if these terms can be estimated, then budget calculations may give valuable insight into the important mechanisms affecting moisture transport in the LLJ. We will explore the use of satellite estimates of anvil-top

divergence to provide some measure of the convective vertical transport within the domain, and the high-resolution models and airborne DIAL/HRDL systems also will provide vertical eddy fluxes of moisture.

Acknowledgments. This work was completed with funding from the United States Weather Research Program (USWRP). We thank Susan Carsten and Ed Szoke for helpful reviews.

6. REFERENCES

Anderson, C. J. and R. W. Arritt, 2001: Representation of summertime low-level jets in the Central United States by the NCEP-NCAR reanalysis. *J. Climate*, **14**, 234-247.

Augustine, J. A. and F. Caracena, 1994: Lower tropospheric precursors to nocturnal MCS development over the central United States. *Wea. Forecasting*, **9**, 116-135.

Brill, K. F., L. W. Uccellini, R. P. Burkhart, T. T. Warner, and R. A. Anthes, 1985: Numerical simulations of a transverse indirect circulation and low-level jet in the exit region of an upper-level jet. *J. Atmos. Sci.,* **42**, 1306-1320.

Browning, K. A., and C. W. Pardoe, 1973: Structure of low-level jet streams ahead of mid-latitude cold fronts. *Quart. J. Roy. Met. Soc*., **99**, 619-638.

Fritsch, J. M., R. J. Kane, and C. R. Chelius, 1986: The contribution of mesoscale convective weather systems to the warm-season precipitation in the United States. *J. Climate Appl. Meteor.*, **25**, 1333-1345.

Guo, Y.-R., Y.-H. Kuo, J. Dudhia, D Parsons, and C. Rocken, 2000: Four-dimensional variational data assimilation of heterogeneous mesoscale observations for a strong convective case. *Mon. Wea. Rev.*, **128**, 619-643.

Higgins, R. W., Y. Yao, E. S. Yarosh, J. E. Janowiak, and K. C. Mo, 1997: Influence of the Great Plains low-level jet on summertime precipitation and moisture transport over the central United States. *J. Climate*, **10**, 481-507.

Hock, T. F., and J. L. Franklin, 1999: The NCAR GPS dropwindsonde. *Bull. Amer. Meteor. Soc.*, **80**, 407-420.

Hoecker, W. J. Jr.,1963: Three southerly low-level jet systems delineated by the weather bureau special pibal network of 1961. *Mon. Wea. Rev.*, **10**, 573-582.

Koch, S. E., D. Hamilton, D. Kramer, and A. Langmaid, 1998: Mesoscale dynamics in the Palm Sunday tornado outbreak. *Mon. Wea. Rev.*, **126**, 2031-2060.

Kuo, Y.-H., and R. A. Anthes, 1984: Accuracy of diagnostic heat and moisture budgets using SESAME-79 field data as revealed by observing systems simulation experiments. *Mon. Wea.. Rev.*, **112**, 1465-1481.

Roads, J. O., S. C. Chen, A. Guetter, and K. Georgakakos, 1994: Large-scale aspects of the United States hydrologic cycle, *Bull. Amer. Met. Soc*., **75**, 1589-1610.

Uccellini, L. W., R. A. Petersen, K. F. Brill, P. J. Kocin, and J. J. Tuccillo, 1987: Synergistic interactions between an upper-level jet streak and diabatic processes that influence the development of a low-level jet and a secondary coastal cyclone. *Mon. Wea. Rev.*, **115**, 2227-2261.

Weckwerth, T. M., D. B. Parsons, S. E. Koch, J. A. Moore, M. A. Lemone, B. B. Demoz, C. Flamant, B. Geerts, J. Wang, and W. F. Feltz, 2004: An overview of the international H_2O Project (IHOP 2002) and some preliminary highlights. *Bull. Amer. Meteor. Soc.*, **85** (in press).